Swiss J Geosci (2013) 106:161–177
DOI 10.1007/s00015-013-0143-7

New coelacanth material from the Middle Triassic of eastern Switzerland, and comments on the taxic diversity of actinistans

Lionel Cavin · Heinz Furrer · Christian Obrist

Received: 1 February 2013 / Accepted: 9 August 2013 / Published online: 16 November 2013

Abstract New coelacanth material from the Middle Triassic Prosanto Formation of the Ducan and Landwasser area near Davos in eastern Switzerland, Canton Graubünden, is described. A sub-complete individual is visible in ventral view, and shows details of its branchial apparatus. In particular, it possesses relatively large teeth on the ceratobranchials, and possible ossified hypobranchials. Few diagnostic characters are observable, and most of them are visible on the mandibles preserved in lateral view. This specimen shares characters with *Ticinepomis peyeri*, a smaller form from the Middle Triassic of Monte San Giorgio, whose holotype is re-described in part here. A second specimen, a fragmentary caudal skeleton shows the typical supplementary lobe of coelacanths, and meristic characters indicating probable close affinities with *T. peyeri*. We refer this material to *Ticinepomis* cf. *T. peyeri.* Because the new specimen is larger than the holotype, we refute the possible juvenile status of the small specimen from Monte San Giorgio. The new material of *Ticinepomis* from Canton Graubünden shows anatomical features not preserved on the holotype and allows the addition of new characters to a previously published data matrix of actinistians. A phylogenetic analysis is performed, which supports that *Ticinepomis* is nested among the Latimeriidae. The diversity of post-Palaeozoic coelacanths is assessed. The taxic diversity of observed occurrences shows a peak in the Early Triassic and a peak in the Late Jurassic, as detected in previous studies. When ghost lineages are included in the computation, the Late Jurassic peak is smoothened. By comparing the taxic diversity curves with the curve of average ghost lineage duration, we conclude that the Early Triassic peak of diversity was probably caused by a biological radiation, whereas the Late Jurassic peak of observed diversity is probably the result of a Lagerstätten effect.

Keywords Prosanto Formation · Ladinian · Phylogeny · Taxic diversity · Branchial apparatus

Editorial handling: D. Marty.

Electronic supplementary material The online version of this article (doi:10.1007/s00015-013-0143-7) contains supplementary material, which is available to authorized users.

L. Cavin (✉)
Department of Geology and Palaeontology, Muséum d'Histoire Naturelle, CP6434, 1211 Geneva 6, Switzerland
e-mail: Lionel.Cavin@ville-ge.ch

H. Furrer
Paläontologisches Institut und Museum der Universität Zürich, Karl Schmid-Strasse 4, 8006 Zurich, Switzerland

C. Obrist
Erliackerweg 8, 4462 Rickenbach, BL, Switzerland

Institutional and anatomical abbreviations

PIMUZ	Collection of the Palaeontological Institute and Museum, University of Zürich
Ang	Angular
a.Pa	Anterior parietal
Apal	Autopalatine
Art	Articular
art.fa	Articular facet
ax.mes	Axial mesomeres
Bb	Basibranchial
b.fen	Basicranial Fenestra
Boc	Basioccipital
Bs	Basisphenoid
Cb	Ceratobranchial (numbered)
Ch	Ceratohyal
Cl	Cleithrum

Cla	Clavicle
Co	Coronoid (numbered)
De	Dentary
Dpal	Dermopalatine
d.p	Enlarged sensory pore within dentary
D1.b	Basal bone of the first dorsal fin
d1.f	First dorsal fin
D2.b	Basal bone of the second dorsal fin
d2.f	Second dorsal fin
Ecl	Extracleithrum
Exo	Exoccipital
f.pop.sc	Foramen for the preopercular sensory canal
f.VII.m.ext	External mandibular ramus of the VII
Gu	Gular
h.a + s	Haemal arch and spine
Hb	Hypobranchial
Ih	Interhyal
n.a + s	Neural arch and spine
Op	Opercle
ot.sh	Otic shelf
Part	Prearticular
Pb	Pharyngobranchial
P.b	Pelvic bone
P.Co	Principal coronoid
Pmx	Premaxilla
Ppa	Postparietal
p.Pa	Posterior parietal
Pop	Preopercle
Ps	Parasphenoid
Pt	Pterygoid
p.w.Pro	Posterior wing of the prootic
pec.f	Pectoral fin
Q	Quadrate
Ra	Radial
Rart	Retroarticular
ros.m	Median rostral
ros.l	Lateral rostral
Sb	Suprapharyngobranchial
Sc	Scale
Scc	Scapulocoracoid
s.l.c.f	Supplementary lobe of the caudal fin
So	Supraorbital
Sop	Subopercle
sop.br	Subopercular branch of the preopercular canal
Spl	Splenial
Stt	Supratemporal
Sy	Symplectic
T	Tooth
t.p.Bb	Basibranchial tooth plates
t.p.Cb	Ceratobranchial tooth plates
Uhy	Urohyal
v.pr.Pa	Ventral process of the posterior parietal
IX	Glossopharyngeal foramen
(l) and (r)	Refer to ossifications from the left and right side of the specimen, respectively

1 Introduction

Coelacanths form a clade of sarcopterygian fishes known from the Early Devonian (Johanson et al. 2006) up to the present day (Smith 1939), with a long fossiliferous gap during the whole Cenozoic. The group is known for its evolutionary conservatism and studies have shown that coelacanths reached their peak of taxic diversity during the Early Triassic (Cloutier 1991; Forey 1998; Schultze 2004; Wendruff and Wilson 2012). In the Middle Triassic, the diversity was still proportionally high, with 6 species according to Forey (1998) and 12 species according to Schultze (2004) (the difference is due to the way authors assessed species status), plus some new species described from 2004. In Europe, the properly-defined Middle Triassic species are *Alcoveria brevis* Beltan, 1972, from Spain; *Garnbergia ommata* Martin and Wenz, 1984 and *Hainbergia granulata* Schweizer, 1966, both from Germany; *Heptanema paradoxum* Bellotti, 1857, from Italy and *Ticinepomis peyeri* Rieppel, 1980, from Switzerland. The latter species has been described on the basis of a specimen discovered in the famous Middle Triassic locality of Monte San Giorgio in Ticino, Switzerland (Rieppel 1980). In 1985, Rieppel described fragments of a larger coelacanth from Monte San Giorgio, which he referred to cf. *Holophagus picenus* (*Undina picenus* according to Rieppel, 1980 and *Undina picena* according to Forey, 1998). Outside Europe, Middle Triassic coelacanths have been recorded in the USA with *Moenkopia wellesi* Schaeffer and Gregory, 1961, and recently in China with *Luopingcoelacanthus eurylacrimalis* and *Yunnancoelacanthus acrotuberculatus* (Wen et al. 2013).

Here, we describe new coelacanth material of *Ticinepomis* cf. *T. peyeri* from the Middle Triassic Prosanto Formation of the Canton Graubünden. Characters of these new specimens, together with new observations on the type specimen of *T. peyeri* and new information from recently described coelacanths, allow us to perform a new phylogenetic analysis, and to discuss the taxic diversity pattern of post-Palaeozoic coelacanths.

2 Geology, stratigraphy and palaeoenvironment

Since 1989, systematic prospecting and excavations in the Middle Triassic Prosanto Formation by a team of the Zürich University and volunteers directed by one of us (H.F.)

provided a rich fauna of well-preserved vertebrate and invertebrate fossils from this Fossil Lagerstätte (Bürgin et al. 1991; Furrer 2009). The assemblage comprises plants, invertebrates such as bivalves, gastropods, and crustaceans, as well as vertebrates including fish and reptiles. Among the fishes, ray-finned fishes (Actinopterygii) are represented by saurichthyiforms, peltopleuriforms, perleidiforms, ginglymodians and halecomorphs (Arratia and Herzog 2007; Bürgin 1999; Bürgin and Herzog 2002; Bürgin et al. 1991; Herzog 2001, 2003a, b).

A first fragment of a coelacanth, consisting of an articulated caudal fin, was found in 1992 during the first systematic excavation in the main fish beds of the upper Prosanto Formation at the locality Strel (2,580 m a.s.l.), located 10 km SW of Davos. The second specimen, a sub-complete fish, was discovered in 2006 by one of us (C.O.) in the middle part of the Prosanto Formation at site DF 10 (2,750 m a.sl.l.) near the Ducanfurgga, 13 km south of Davos.

The Prosanto Formation of the eastern Swiss Alps is formed by a 100–200 m thick sequence of dark limestones, shales and dolomites. Overlying the Vallatscha and underlying the Altein formations, the Prosanto Formation extends for more than 20 km as a lenticular intercalation in shallow water dolomites that are part of the strongly deformed sediments of the Austroalpine Silvretta Nappe near Davos (Figs. 1, 2; Furrer et al. 1992). The diverse fauna and flora of sauropterygian reptiles, fishes, molluscs, crustaceans, marine and terrestrial plants (e.g. Bürgin et al. 1991; Furrer 1995, 2009) in the Prosanto Formation shares many similarities with the classic Late Anisian/Early Ladinian Monte San Giorgio Fossil Lagerstätten in the Southern Alps (Besano and Meride formations). A recent U/Pb zircon age of 240.91 ± 0.26 Ma from a volcanic ash layer in the fossiliferous beds of the upper Prosanto Formation from a well exposed section ESE of Ducanfurgga (Furrer et al. 2008) suggests a good time correlation with the vertebrate horizons in the lower Meride Formation of the Southern Alps (Gredleri Zone, Early Ladinian; Stockar et al. 2012).

The rich and well-preserved actinopterygian fish fauna suggests a deposition in stagnant abiotic, probably anoxic bottom water conditions of a small intraplatform basin (Furrer 1995). Small plankton feeding fishes such as *Habroichthys*, large predator fishes such as *Saurichthys*, and also the rare sauropterygian reptiles probably lived in the surface water. Medium-sized fish preying on hard-shelled bivalves and crustaceans, but also calcareous algae must have lived at the border of the basin in a shallow water and oxygenated environment. Echinoderms (echinoids and holothurians), and cephalopods (ammonoids) are very rare, suggesting euryhaline surface water of a restricted basin (Furrer 2009). Terrestrial plants (Grauvogel-Stamm et al. 2003), a few insects, a fragment of a rauisuchian reptile (Scheyer and Desojo 2011), and two fragmentary but articulated remains of another terrestrial tetrapod, *Macrocnemus* (Fraser and Furrer 2013) must have been washed in.

3 Materials and methods

The material under study consists of a sub-complete specimen preserved on a slab of dark limestone, and a caudal fin in dark marlstone. The caudal fin was prepared only mechanically with thin steel needles under the microscope at the Palaeontological Institute and Museum, University of Zürich (PIMUZ). The preparation of the sub-complete specimen was done mechanically with an air tool, thin steel needles and sand blaster all under the microscope, completed by chemical treatment with diluted acetic acid totaling 240 h of work by one of us (C.O.). We took X-ray photographs of the branchial apparatus in order to detect more details, but it was unsuccessful. The fossils are stored in the collection of PIMUZ. Osteological nomenclature used in the descriptive part follows Forey (1998).

The parsimony analysis was run in PAUP* 4.0b10 (Swofford 2001). A heuristic search (using random addition sequence, replicated 10,000 times, 1 tree held at each iteration, and tree bisection and reconnection branch swapping) was carried out to try to avoid the 'islands of trees' problem (Maddison 1991).

For analyzing the diversity of coelacanths through time, we plotted the amount of observed genera for each epoch of the Late Permian–Recent time interval ('observed diversity'). Only genera that are included in the phylogenetic analysis are considered. We also constructed a diversity curve that includes for each time bin, in addition to the observed genera, the Lazarus taxa and the amount of inferred ghost lineages ('total diversity'). The ghost lineage is the amount of stratigraphic range of a taxon that must be added to comply with a phylogenetic tree. It is based on the assumption that the lineage of the oldest known occurrence of a clade should be as old as the oldest occurrence of its sister clade. In order to assess if the observed rises in generic diversity are caused by real biological phenomena or if they are due to a better sampling (Lagerstätten effect), we used the method proposed by Cavin and Forey (2007). This method involves calculating the average ghost lineage of the genera observed in each time bin. If this average duration is low or drops at the same time that taxic diversity raises, this indicates the occurrence of a biological radiation (most of the observed taxa are at the top of short branches); if a peak of diversity is not associated with a drop in average ghost duration, we can suspect that a Lagerstätten effect is at the origin of the peak (most of the observed taxa are at the top of long branches) (Cavin and Forey 2007).

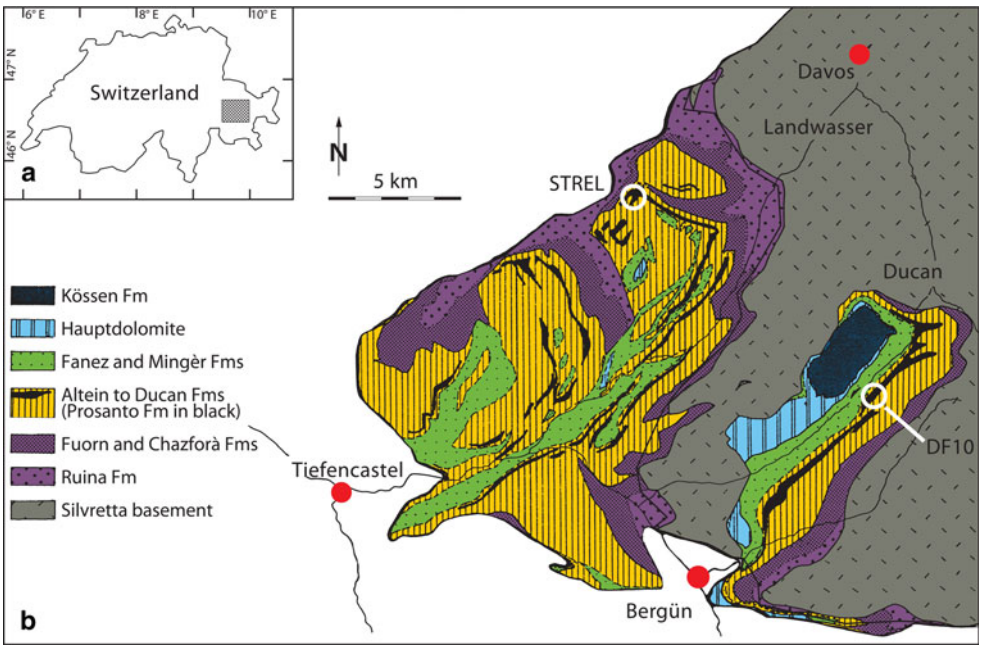

Fig. 1 **a** Geographical setting; **b** Geological map of the Austroalpine Silvretta Nappe in the Ducan–Landwasser area near Davos, Canton Graubünden, eastern Switzerland. Fossil sites Ducanfurgga 10 (DF 10) and Strel

4 Systematic palaeontology

Subclass Sarcopterygii Romer, 1955
Infraclass Actinistia Cope, 1891
Suborder Latimerioidei sensu Dutel et al. 2012
Family Latimeriidae sensu Dutel et al. 2012

Genus *Ticinepomis* Rieppel, 1980

Emended diagnosis (*modified from Forey* 1998). Monotypic latimeriid coelacanth characterised by the following set of characters (*indicates character states regarded as derived within the latimeriids): postparietal shield short, less than half the length of the parietonasal shield; opercle relatively large and rounded; premaxilla bears four stout, conical teeth; dentary shows a pronounced ventral edge midway along its length*; splenial large and curved*; palatoquadrate deep throughout with the pterygoid showing a deep anterior limb*; ornament upon the opercle, preopercle and roofing bones consists of rounded tubercles and some ridges; cleithrum expanded dorsally; basal plate of D1 is approximately triangular; all the fin rays of the median fins are expanded to some degree*; denticles borne upon the anterior rays of both D1 and the caudal fin.

Type species Ticinepomis peyeri Rieppel, 1980

Diagnosis (*from Forey* 1998). $D_1 = 8$; $D_2 = 22–23$; C = 18/18; P => 17; abdominal vertebrae = 33; caudal vertebrae = 18.

Material. Holotype (PIMUZ T 3925), a sub-complete fish on part and counterpart (Fig. 3)

Description. The holotype was described by Rieppel (1980) and here we focus only on osteological structures, whose interpretation differs from the original description. Rieppel (1980) recorded the occurrence of both autopalatines, while we recognise the left one only (Fig. 3a, Apal). We agree with the probable presence of an elongated right posterior parietal ('posterior frontal' of Rieppel) on the part (Fig. 3a, p.Pa(r)), and we recognised on the counterpart the left posterior parietal (Fig. 3b, p.Pa(l)), which corresponds to what Rieppel (1980) labelled 'left posterior frontal' and basisphenoid. A well-developed ventral process of the posterior parietal is visible in ventral view on the part (Fig. 3a, v.pr.Pa). In our interpretation of the specimen, the ventral part of the basisphenoid is visible on the part (Fig. 3a, Bs) and corresponds to the posterior part of the bone labelled 'metapterygoid' by Rieppel (1980) and regarded as the antotic articulation by him. It is lined ventrally by a fragment of the parasphenoid (Fig. 3a, Ps), which extends anteriorly underneath the suspensorium as indicates the presence of a strong ridge. The interpretation of the skull roof of the postparietal shield differs from Rieppel's interpretation. We identify on the counterpart a right postparietal (Fig. 3b, Ppa(r)), incomplete, and a right supratemporal tapering posterolaterally (Fig. 3b, Stt(r)) (these ossifications were regarded by Rieppel (1980) as a compound postparietal-supratemporal and as an extracapsular, respectively,

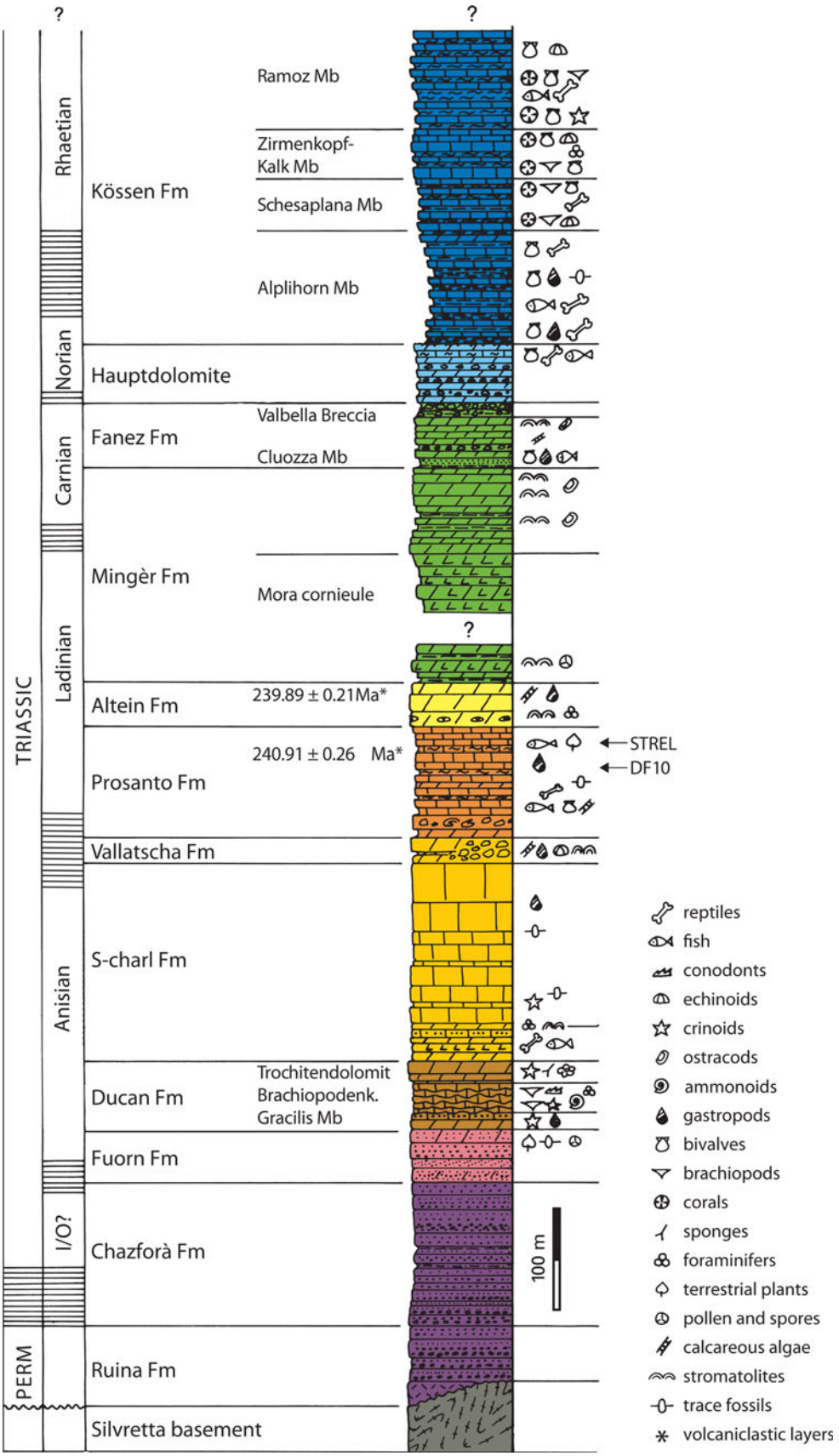

Fig. 2 Stratigraphical section of the Austroalpine Silvretta Nappe in the Ducan–Landwasser area near Davos, Canton Graubünden. Uncertainty of stage boundaries are marked by *horizontal lines* in the *left column*

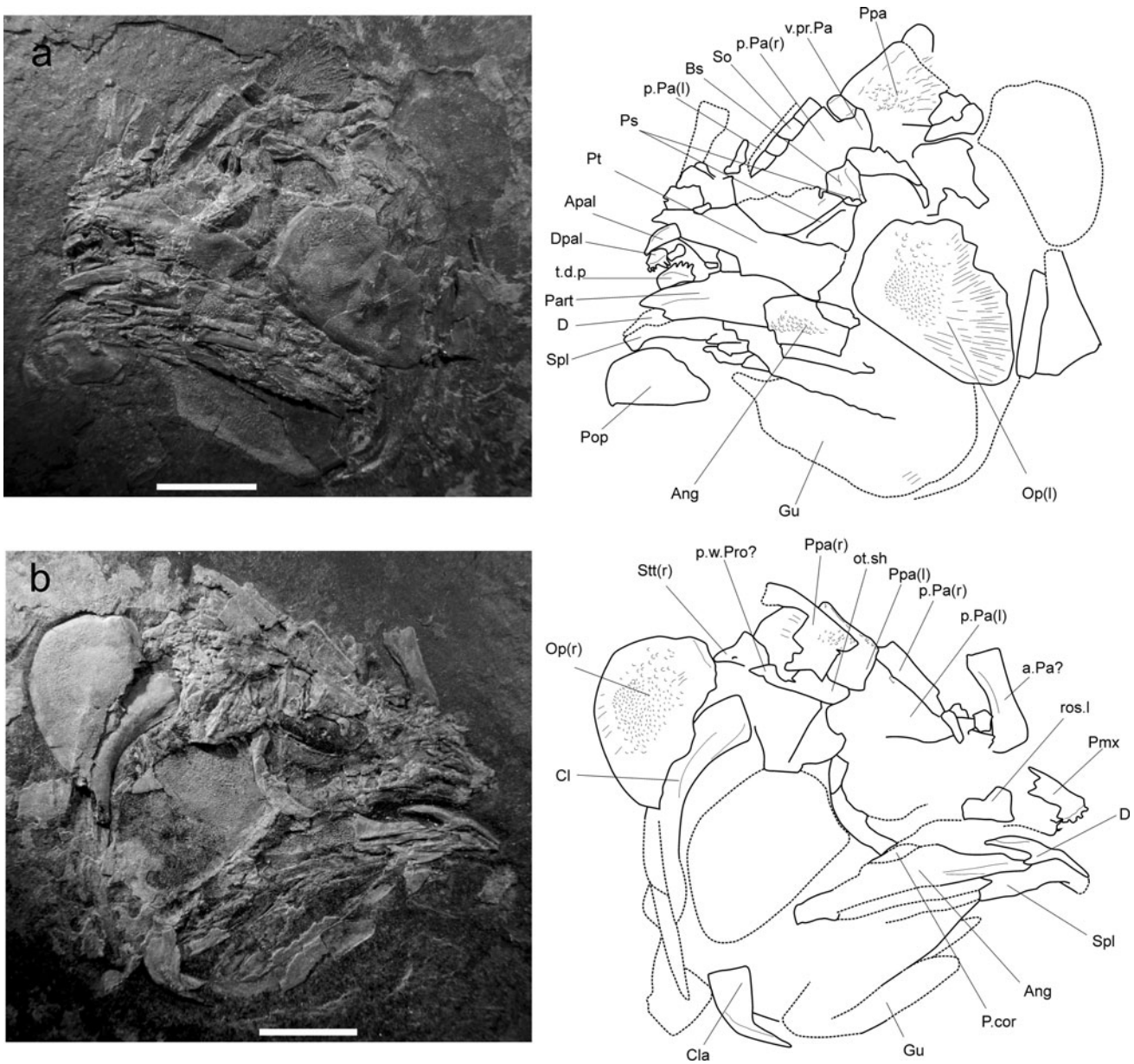

Fig. 3 *Ticinepomis peyeri*, holotype (PIMUZ T 3925), Monte San Giorgio, upper part of the Besano Formation (Grenzbitumenzone), Middle Triassic (Early Ladinian) of Canton Ticino. **a** Part. **b** Counterpart. *Scale bars* 10 mm

based on the nomenclature used here.) Underneath these elements is the left postparietal (Fig. 3b, Ppa(l)), which also shows its external surface. The fact that external faces of both left and right bones of the skull roof of the postparietal shield face to the right side of the specimen, on the counterpart, indicates that the skull roof should have been crushed in a way that shifted the median edges of the left ossifications ventrally. The external side of the postparietals are ornamented with tubercles in the anterior and central regions, and with anteroposterior ridges in the posterior region. Ventral to the right postparietal, and fused to it, we identified the prootic with a rounded otic shelf (Fig. 3b, ot.sh) extending anteriorly and a posterior extension possibly representing the posterior wing (Fig. 3b, p.w.Pro). The prootic was regarded as part of the postparietal ('parietal') by Rieppel (1980).

Rieppel (1980, fig. 3) figured on a tentative reconstruction of *T. peyeri* a large opening in the lower jaw between the dentary and the angular, which could be regarded as a large dentary pore for the dorsal branch of the mandibular canal. However, this space corresponds to a notch in the dentary that was filled up medially with the prearticular in a manner similar to what was reconstructed in *Whiteia woodwardi* (Forey 1998, fig. 4.15).

We agree with Rieppel's (1980) description of other cranial and post-cranial elements of the holotype specimen.

4.1 *Ticinepomis* cf. *T. peyeri*

Material. One sub-complete specimen (PIMUZ A/I 2985) from the site DF 10 near Ducanfurgga found in the middle Prosanto Formation (Early Ladinian). The fossil displays the head, visible in ventral view, and the anterior portion of the vertebral column with both dorsal fin supports still in place (Figs. 4, 5, 6). The posterior part of the axial skeleton is shifted and mostly disarticulated.

One isolated caudal fin (PIMUZ A/I 1959) from the locality Strel, found in the upper Prosanto Formation

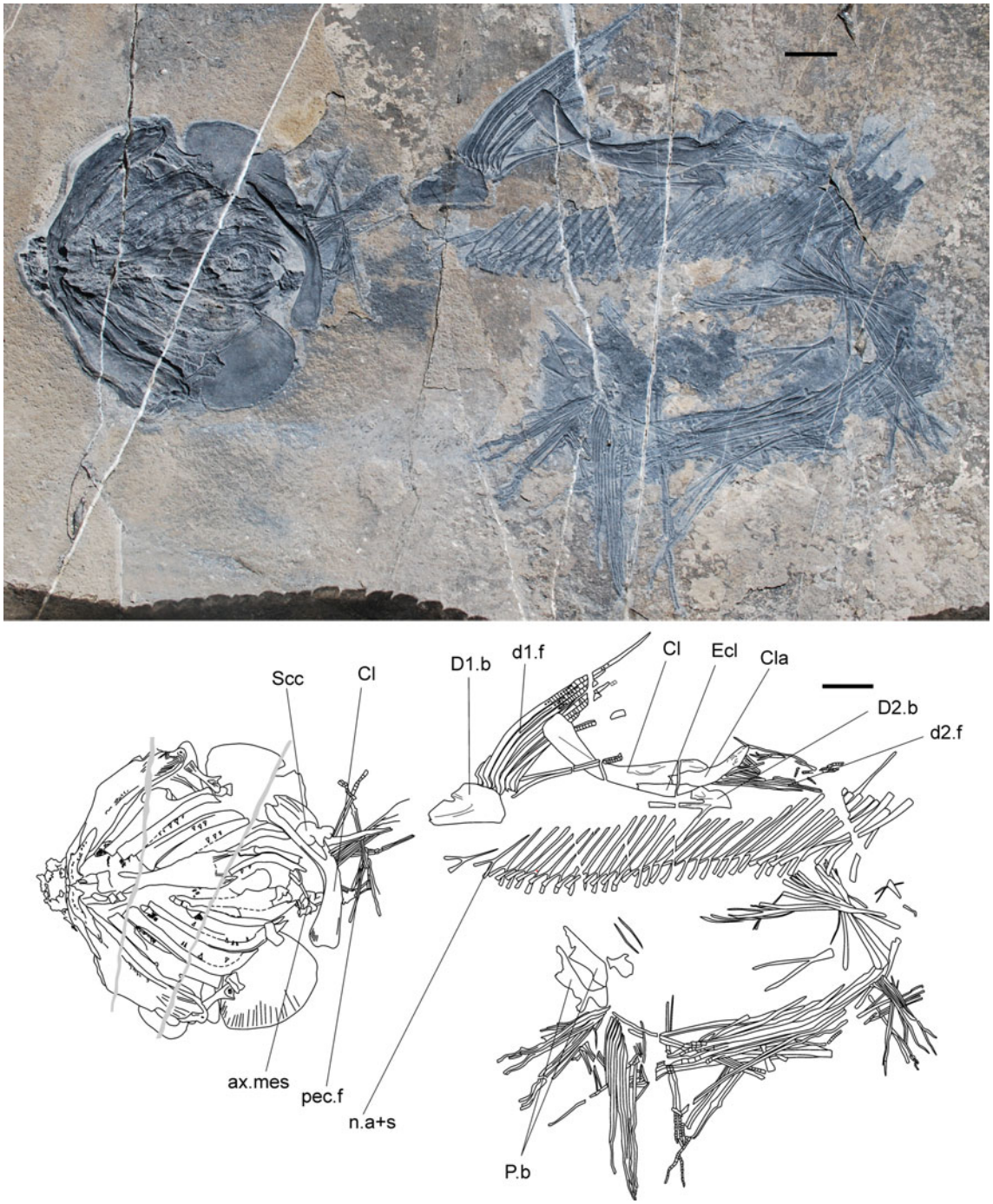

Fig. 4 *Ticinepomis* cf. *T. peyeri*, sub-complete specimen (PIMUZ A/I 2985), Ducanfurgga 10, middle part of the Prosanto Formation, Middle Triassic (Early Ladinian) of Canton Graubünden. *Scale bars* 20 mm

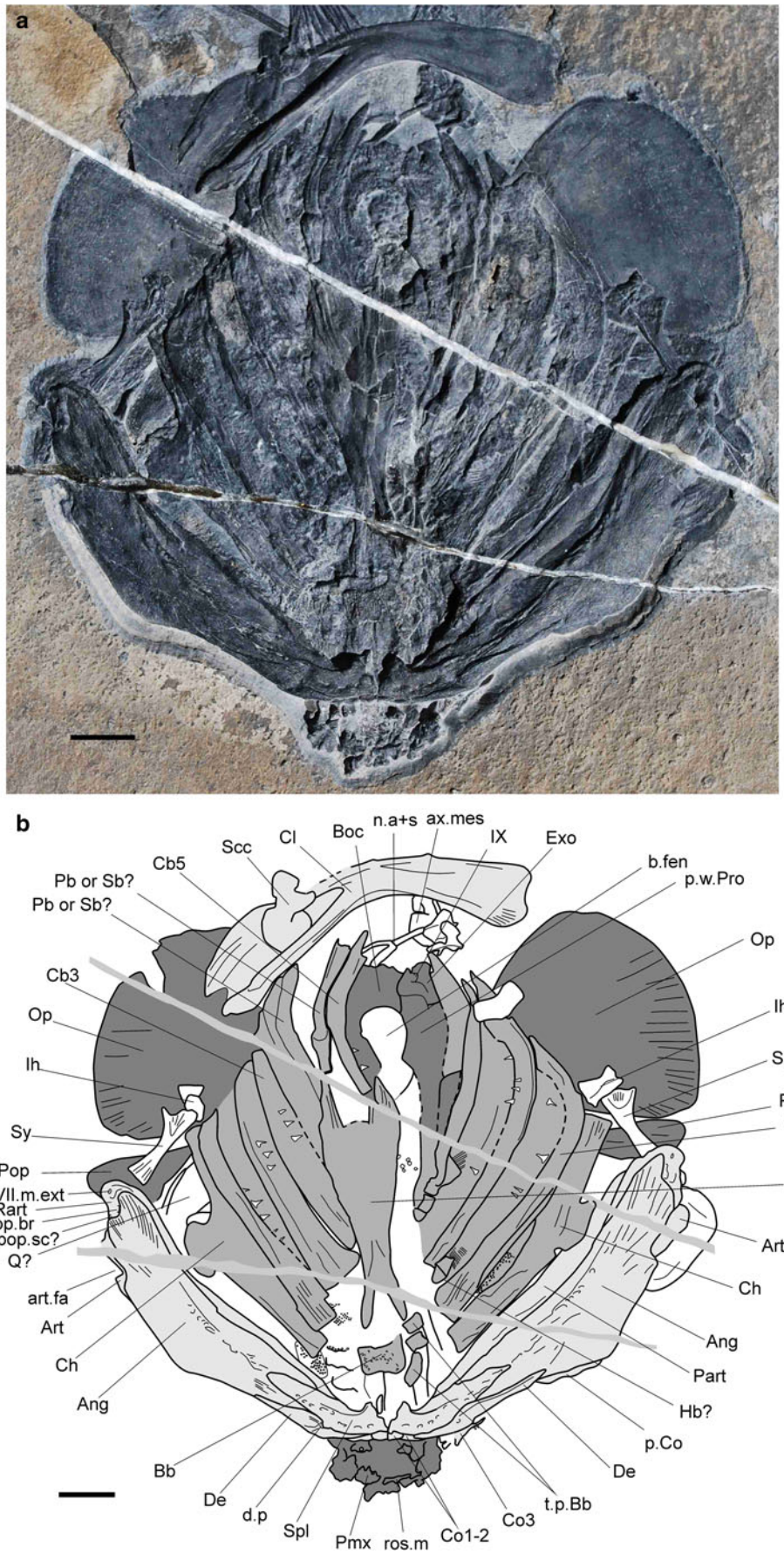

Fig. 5 *Ticinepomis* cf. *T. peyeri*, detail of the head of the sub-complete specimen (PIMUZ A/I 2985) in ventral view, Ducanfurgga 10, middle part of the Prosanto Formation, Middle Triassic (Early Ladinian) of Canton Graubünden. **a** Photograph. **b** Drawing: *light grey* mandibles and pectoral girdle; *intermediate grey* branchial apparatus; *dark grey* braincase, snout and opercular series. *Scale bars* 10 mm

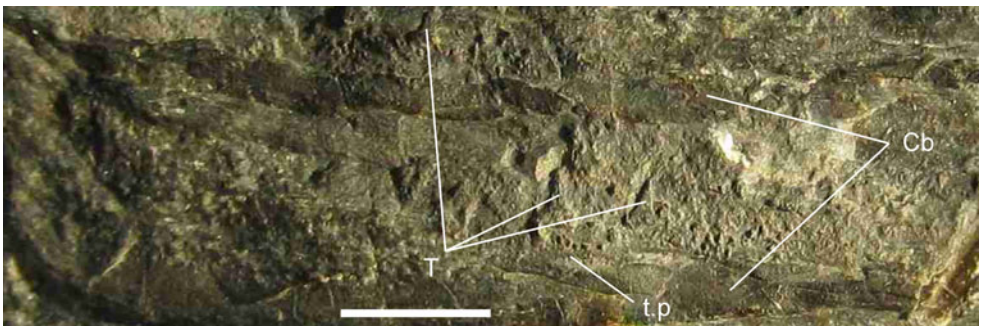

Fig. 6 *Ticinepomis* cf. *T. peyeri*, detail of two ceratobranchial with branchial teeth of the sub-complete specimen (PIMUZ A/I 2985), Ducanfurgga 10, middle part of the Prosanto Formation, Middle Triassic (Early Ladinian) of Canton Graubünden. *Scale bar* 5 mm

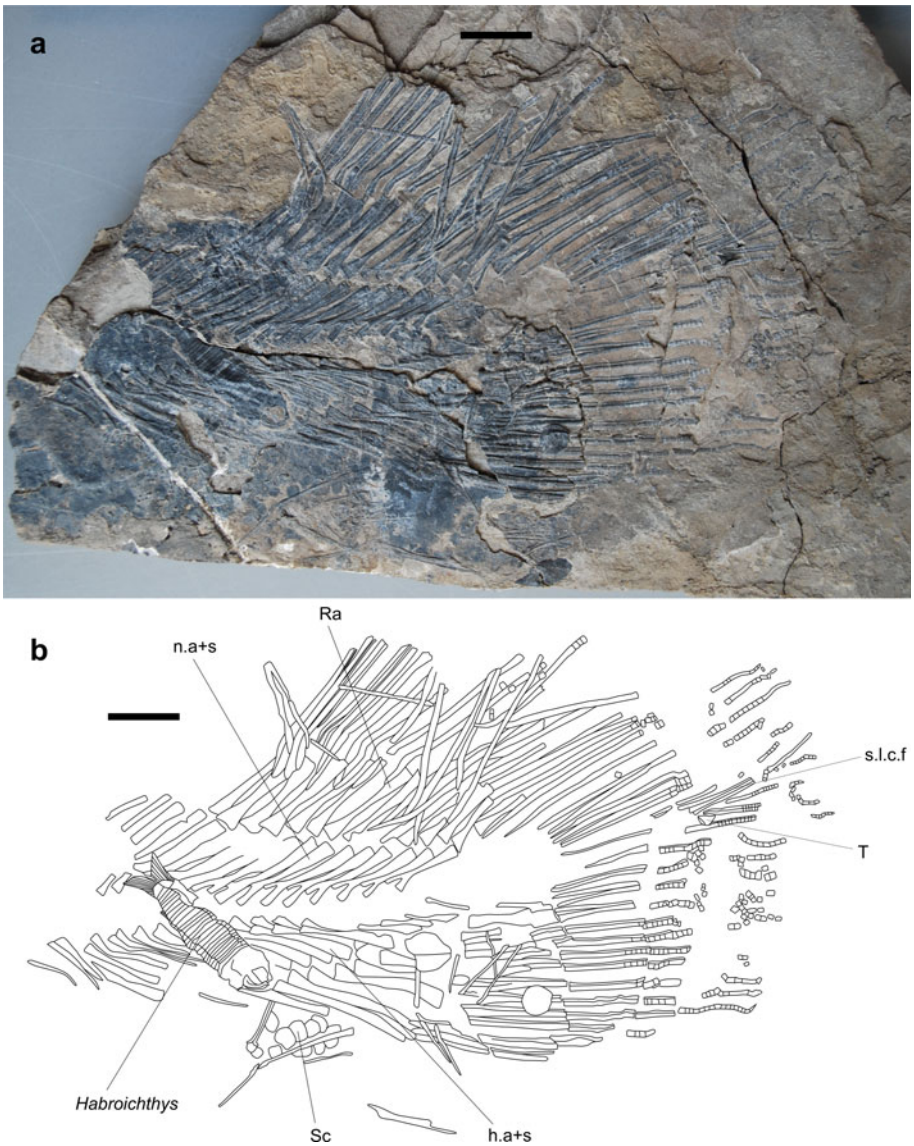

Fig. 7 *Ticinepomis* cf. *T. peyeri*, caudal skeleton, (PIMUZ A/I 1959), Strel, upper part of the Prosanto Formation, Middle Triassic (Early Ladinian) of Canton Graubünden. **a** Photograph. **b** Drawing. *Scale bar* 10 mm

(Early Ladinian); with a specimen of the ray-finned *Habroichthys* lying above the vertebral column, and a probable tooth of *Saurichthys* above the supplementary lobe (Fig. 7).

4.1.1 Description of PIMUZ A/I 2985

The head, including the branchial apparatus, opercular series and lower jaw, is visible in ventral view (Figs. 4, 5).

Both lower jaws have been shifted laterally and expose their lateral side. The left pectoral girdle has slightly shifted but is still located just behind the opercular bones, while the right one is posteriorly displaced, behind the level of the first dorsal fin. The anteriormost part of the vertebral elements are missing, whereas the abdominal vertebral elements are preserved in anatomical position from the level of the first dorsal fin and extend past the second dorsal basal plate. The remaining part of the axial skeleton is mostly disarticulated and bent at 180°, the caudal portion pointing anteriorly.

Skull roof and braincase (Fig. 5). Because of the mode of preservation of the specimen, the skull roof is unknown except the tip of the premaxilla (Fig. 5, Pmx) and a medial rostral (Fig. 5, ros.m), which are both visible in ventral view. The left premaxilla bears two large teeth and fragments of two smaller ones. Of the braincase, only the posterior extremity is partly visible. In the otico-occipital portion, the basicranial fenestra (Fig. 5, b.fen) forms a regular curved posterior margin. Posterior to the fenestra is the basioccipital (Fig. 5, Boc), which is almost as long as wide in ventral view. Along the posterior part of the right margin of the basioccipital is the exoccipital (opisthotic) (Fig. 5, Exo), which is pierced by a foramen for the glossopharyngeal foramen (IX) and excavated on its posterior margin by a notch, possibly for the vagus nerve (X). Lateral to the basicranial fenestra lies the posterior wing of the prootic (Fig. 5, p.w.Pro). Other elements of the otico-occipital portion of the braincase are hardly recognizable and nothing from the ethmosphenoid portion is visible. Although both portions of the skull are not entirely visible, an approximation of the length of the otico-occipital portion indicates that it is significantly shorter than the estimated length of the ethmosphenoid portion, probably less than half.

Cheek bones and opercular series. From the bones covering the cheek and opercular region, only the opercles (Fig. 5, Op) and preopercles (Fig. 5, Pop) are visible. Both opercles, observable in internal view, are ovoid ossifications, with an almost straight dorsal margin and gently curved anterior and posterior margins. This shape of opercle is more rounded than in most coelacanths, in particular in cf. *H. picenus* described from Monte Giorgio (Rieppel 1985), but it looks like the opercle of *T. peyeri*. On both sides of the head and located anteriorly to the anteroventral edge of the opercles are triangular ossifications with rounded posteroventral corners regarded as preopercles because of their location and because of their shape, which is deeper than long.

Lower jaw. Both lower jaws are visible in lateral view. Most of the lateral side of the jaw is covered by the angular (Fig. 5, Ang; Fig. 8b). The ossification is ornamented with faint ridges, more noticeable along its posterior margin. At its mid-length, the oral margin of the angular marks an angle. Anterior to the angular is the splenial (Fig. 5, Spl; Fig. 8b), which develops an elongated process extending posteriorly and being capped by the angular. This peculiar arrangement is reminiscent of the arrangement observed in *Whiteia*, in *Diplurus* (Forey 1998: figs. 5.9A and 4.16A, respectively), and in *Ticinepomis* (Rieppel 1980, fig. 3). The splenial marks a strong angle in its anterior extremity, especially visible on its ventral margin. This angle may be accentuated by the flatten condition of the specimen, but the shape of the ossification clearly show that the curvature is more developed than in most other coelacanths. *Ticinepomis peyeri* is the only coelacanth that shows an angle almost as marked as in our specimen (Fig. 8). A small process is present at the anteroventral corner of the ossification. The dentary (Figs. 5d, 8b) is visible as a thin splint-like angled ossification bordering dorsally along the anterior extremity of the angular as well as most of the splenial. The principal coronoid (Fig. 5, p.Co following Forey's nomenclature 1998; Fig. 8b) is visible on the right jaw as a shallow ossification, which lines the angular anterior to the dorsal angle of the bone, but the complete shape of the bone can not be determined. Although the principal coronoid may

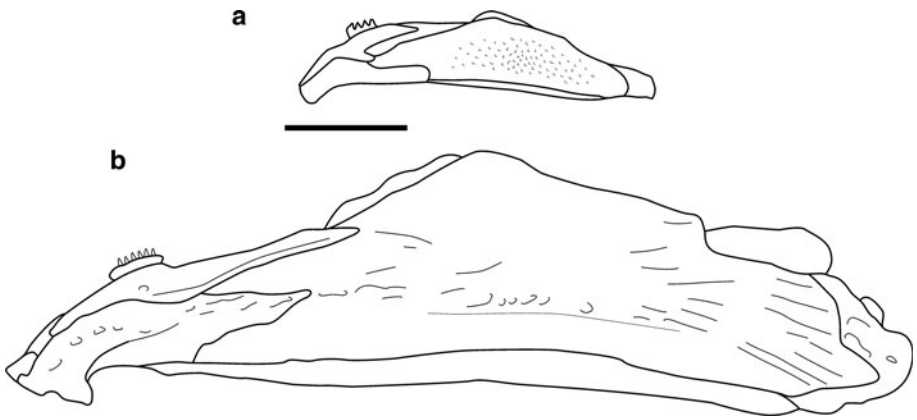

Fig. 8 Comparison between the reconstructed left lower jaws of **a** *Ticinepomis peyeri*, based on the holotype (PIMUZ T 3925) and **b** the sub-complete specimen (PIMUZ A/I 2985) *Ticinepomis* cf. *T. peyeri*. *Scale bar* 10 mm

have shifted after death, it is unlikely that the ossification was protruding as much as in *Latimeria*. Such a small and apparently shallow principal coronoid is present in *Ticinepomis* (Fig. 8a). Two small bones located anteriorly to the dentary and close to the symphysis are probable coronoids (Fig. 5, Co1-2; Fig. 8b), although no teeth are visible. Another coronoid, with two pointed teeth, has slightly shifted from the right jaw (Fig. 5, Co3; Fig. 8). The total number of coronoids was four, including the principal one. A small part of the articular (Fig. 5, Art; Fig. 8b) is visible and rises above the angular, where it forms the anterior part of the articular facet for the quadrate. The posterior margin of the jaw is occupied by the retroarticular (Fig. 5, Rart; Fig. 8b), which is caped by the posterior extremity of the angular. The posterior extremity of the jaw shows several pores, which can be interpreted as follows: a tiny pore, located close to the posterior margin of the retroarticular, accommodated the external mandibular ramus of the VII (Fig. 5, f.VII.m.ext), and a larger and elongated pore, which opens at the limit between the retroarticular and angular, corresponds to the entrance of the subopercular branch of the preopercular sensory canal (Fig. 5, sop.br). It is not clear, where the main opercular sensory canal enters the mandible, although a small depression visible on the left lower jaw close to the dorsal margin of the retroarticular may represent this pore (Fig. 5, f.pop.sc?). The mandibular sensory canal is more clearly visible on the left jaw: it runs within the angular and has six or seven pore openings above a ridge situated in the middle portion of the angular, then five openings in the posterior part of the splenial, which are separated by a gap from three large pores in the anterior portion of the bone slightly longer on the right hemi-mandible. Dorsally to the gap, at the limit between the splenial and the dentary, is a pore corresponding to the dorsal branch of the mandibular canal (Fig. 5, d.p) present in *Latimeria* and in most extinct coelacanths (Forey 1998).

Branchial arches. The branchial apparatus constitutes most of the visible part of the head and, although the limits of ossifications are often difficult to distinguish because they are crushed, this specimen sheds new light on the gill arches of extinct coelacanths. Elements corresponding to five ceratobranchials are observable on the left side and four only are visible on the right side (Fig. 5, Cb). The ventral edge of the ceratobranchials is excavated by a groove, presumably for the branchial artery like in *Latimeria*. The proximal parts of ceratobranchials are straight, then the ossifications strongly curve at their 3rd quarter and end distally with a blunt spine. The bony structure of the ceratobranchials shows a longitudinally striated pattern but some areas, more or less rounded, present rough surfaces. These may correspond to the tooth plates (Fig. 6, t.p.Ch), for which number and arrangement on each ceratohyal are not fully known. In *Latimeria*, the tooth plates are small and arranged in three rows, and it seems that the tooth plates in PIMUZ A/I 2985 are larger. In *Latimeria*, tiny villiform teeth are borne on rounded tooth plates. On PIMUZ A/I 2985, empty alveoli on the rough surfaces probably indicate the occurrence of similarly shaped teeth. In addition, spaced out and larger teeth, 1.5–2 mm high, conical in shape and with a conspicuous basal support, are preserved sparsely on the ceratobranchials (Figs. 5, 6, T). The larger teeth look similar to the teeth borne on the ceratobranchials of '*Undina pencillata*' (Reis 1888) and *Rhabdoderma elegans* (Forey 1981). *Latimeria* has no hypobranchials, however, in PIMUZ A/I 2985, small ossifications seem to be associated with the bases of the right ceratobranchials 2 and 3 and are regarded, with caution, as ossified hypobranchials (Fig. 5, Hb?). The basibranchial itself does not appear to be preserved on the fossil (it is mostly cartilaginous in *Latimeria*), but fragments of basibranchial tooth plates are preserved (Fig. 5, t.p.Bb). Their arrangement is not clear, but the apparent pattern is at least one large plate in the midline, with three smaller plates laterally at least. This pattern is reminiscent of the basibranchial tooth plates observed in *W. woodwardi* (Forey 1998: fig. 7.6D). The urohyal (Fig. 5, Uhy) has the typical general shape present in coelacanths, i.e. dorso-ventrally flattened with a bifid posterior extremity. In PIMUZ A/I 2985, however, the forked posterior extremity has more tapering processes than in *Macropoma lewesiensis* (Forey 1998, fig. 7.7) and in *Megalocoelacanthus dobiei* (Dutel et al. 2012, fig. 16B), and is more reminiscent to the shape observed in *Latimeria* (Forey 1998, fig. 7.6B). The anterior extremity of the urohyal appears to be deeply forked in PIMUZ A/I 2985, but it is unclear if this corresponds to the genuine shape of the bone or if it is caused by an artifact of preservation.

Pectoral girdle and fins (Figs. 4, 5). The left pectoral girdle is visible in internal view. The cleithrum (Figs. 4, 5, Cl), which consists of ¾ of the entire pectoral girdle, is an arched ossification, with an expanded dorsal extremity. The bone narrows in its angled portion and the ventral arm slightly expands. The scapulocoracoid (Figs. 4, 5, Scc) is visible on the internal side of the left cleithrum. It is an hourglass shaped bone with a proximal spatulated process resting on the internal side of the cleithrum and a distal process dug by an articular facet for the first axial mesomere. The extracleithrum (Fig. 4, Ecl), a coelacanth synapomorphy, is visible still articulated on the lateral side of the right cleithrum: it is a splint-like ossification with a convex posterior margin. An anocleithrum was not observed. The clavicle (Fig. 4, Cla) is still in articulation and its suture with the cleithrum is hardly visible in lateral view. Its horizontal arm is well developed and extends anteriorly. It bears laterally

traces of a ridged ornamentation. Such a distinct horizontal portion of the clavicle is present in *Ticinepomis*, as well as in *Diplurus*, and is regarded as related to the relatively anterior position of the jaw articulation in these two genera (Forey 1998: 119). The pectoral fin endoskeleton is apparently preserved as bony elements located posteriorly to the braincase (Figs. 4, 5, ax.mes). Some shifted rays are present, but their count is not possible.

Pelvic girdle and fins. Both pelvic bones are present and unfused to each other (Fig. 4, P.b). They show the typical posterior, lateral and medial processes present in most coelacanths, but their orientation is uncertain. The medial (?) process extends posteriorly as a wing-like structure. Shifted, elongated fin rays are present not far from the pelvic bones, but it is not clear if they belong to the pelvic or to the caudal fins.

Medial fins. The basal plate of the first dorsal fin (Fig. 4, D1.b) is a large, approximately triangular, ossification with a straight ventral margin, a regularly curved posterior margin and a straight anterior margin dug by a notch. A ridge starting from the anteroventral corner of the bone strengthens the ossification, as in *Ticinepomis* (Rieppel 1980, fig. 5). Eight long segmented and unbranched rays decreasing in length from front to back are still articulating on the basal bone (Fig. 4, d1.f). Several Triassic coelacanth species possess eight rays on the first dorsal fin (see character 96 in the data matrix of the Online Resources). Two small rays precede the first and longest rays. The first long ray is ornamented with small, elongated spines probably arranged along four rows (two rows are visible on a half-ray.) Similar ornamentation is present on the succeeding rays, but it is fainter than on the first one. The half dorsal portions of the elongated rays are segmented.

The basal plate of the second dorsal fin (Fig. 4, D2.b) is composed of a fan-shaped distal part and two elongated processes extending anteriorly and anteroventrally, forming an angle of 50° between each other. No remains of the anal fin are preserved. Most of the distal parts of rays from both dorsal fins are not preserved, except an anterior one on the first dorsal fin, which progressively tapers distally. Posterior rays on the anterior dorsal fin, however, show the beginning of an expanded distal extremity in a similar way to *Holophagus*, *Libys* and *Ticinepomis* (Forey 1998; Dutel et al. 2012).

Vertebral column. 28 neural arches and spines (Figs. 4, 5, n.a + s) are preserved in their original position (plus one shifted and situated very close to the skull), but these do not represent the complete set because the anterior most and posterior most elements are missing. The most anteriorly preserved neural spines are sharp, and they increase in size and broaden distally posteriorly. Circa 12 haemal spines are preserved, but probably more were present in the living fish. They are smaller than their corresponding neural element. No parapophyses and ribs are preserved in the abdominal region.

4.1.2 Description of PIMUZ A/I 1959 (Fig. 7)

Circa 15 caudal vertebrae, represented by the neural (Fig. 7, n.a + s) and haemal (Fig. 7, h.a + s) elements, are preserved anteriorly to the caudal fin. Because the caudal fin is nearly symmetrical in most coelacanths, the orientation of PIMUZ A/I 1959 is unclear. Usually, there are one or two fewer rays in the ventral lobe than in the dorsal one. In PIMUZ A/I 1959, we counted 19 rays in one lobe, which is regarded as the supposedly dorsal lobe, and 14 in the opposite lobe, the ventral one. However, these are the minimum count and it is possible that rays were slightly more abundant on the living fish. As usual in coelacanths, the rays are segmented (except for the first 2 or 3 in the ventral lobe; the situation is not visible in the dorsal one) but unbranched, and there is a one-to-one relationship with the supporting radials (Fig. 7, Ra or 'supraneurals' + radials according to Arratia et al. 2001). The supplementary lobe (Fig. 7, s.l.c.f) is visible as circa eight small rays located at the posterior tip of the caudal fin, between the dorsal and ventral lobes.

Some scales are preserved anteriorly to the ventral lobe of the caudal fin (Fig. 7, Sc). They are worn, but some show a circular pattern, and some present faint ridges probably oriented posteriorly. Rieppel (1980) described packed, elongated blunt or pointed spines on the scales of *T. peyeri*, but instead we observed on the holotype elongated ridges ending posteriorly in short spines. Such spines are not visible in PIMUZ A/I 1959, possibly for preservational reasons.

5 Discussion

5.1 Identification

Although the new specimen PIMUZ A/I 2985 is well preserved and shows a lot of details, its preservational mode renders an identification difficult, because most of the diagnostic characters for coelacanths are present on the skull roof and on the cheek, which are not visible on PIMUZ A/I 2985. Other comparable characters between the holotype of *T. peyeri* and *Ticinepomis* cf. *T. peyeri* described here are present on their lower jaws, which are shown reconstructed in Fig. 8. According to the diagnosis of *Ticinepomis* by Rieppel (1980) and its emended version by Forey (1998), the new specimen is referred to this genus because: (1) the length of the otico-occipital portion is probably less than half the length of the ethmosphenoid portion; (2) the premaxilla bears 4 teeth; (3) the dentary has a pronounced ventral angle midway along its length

(Fig. 8); (4) the cleithrum expands dorsally; (5) the basal plate of D1 is approximately triangular; (6) the distal extremities of the rays of D1 are expanded; and (7) denticles are borne upon the anterior rays of D1. Other characters shared with *T. peyeri*, but not included in the Forey's diagnosis (1998), are: (1) the large size and curved shape of the splenial; (2) the splenial deeper than the dentary (Fig. 8); (3) the rounded shaped opercle and (4) the ornamentation and the horizontal extension of the clavicle (Rieppel 1980). The structure of the caudal fin in PIMUZ A/I 1959 is consistent with the caudal fin of *T. peyeri* described by Rieppel (1980), i.e. 15 segmented rays plus 3 unsegmented rays in both the dorsal and ventral lobe of the caudal fin. However, we cannot see the occurrence of spines on the anterior most rays as described in *T. peyeri*, but this might be caused by a different mode of preservation.

The main difference of PIMUZ A/I 2985 with the type species of *Ticinepomis*, *T. peyeri* is its larger size: *T. peyeri* (PIMUZ T 3925) is circa 180 mm in total length, while we estimate the total length of PIMUZ A/I 2985 to reach circa 615 mm. In that case, the type specimen of *T. peyeri* might be regarded as a juvenile individual, while PIMUZ A/I 2985 would represent an adult stage of the same species. Rieppel (1980: 926) considered that the specimen had reached adult size on the basis of the fusion of the postparietal with the supratemporal, but this condition is no more valid here on the basis of the new interpretation of the postparietal shield of the holotype specimen. A juvenile character of coelacanths is the proportionally longer supplementary lobe of the caudal fin (Schultze 1972; Forey 1981; Anthony and Robineau 1976; Brito and Martill 1999; Cloutier 2010), but unfortunately this feature is not preserved in the type specimen of *T. peyeri*. Another juvenile feature of coelacanths is the late ossification of the basal plates of fins as shown by well-preserved fossils of small individuals of various species, which lack these ossifications (Watson 1927; Schultze 1980; Witzmann et al. 2010). In PIMUZ A/I 2985, the basal plates of the second dorsal and anal fins are not preserved, but the basal plate of the first dorsal, as well as a fragment of the basal plate of the pelvic fin are well-ossified. Another juvenile characteristic has been noted in the caudal fin of very small specimens of *Rhabdoderma exiguum*, in which there is a gap between the neural spines and the supporting radials (or 'supraneurals' + radials), while in larger specimens neural spines and radials are very close (Arratia et al. 2001). Although PIMUZ T 3925 may not be a fully-grown specimen, it seems unlikely that it represents a juvenile specimen because the ossification stage of its skeleton is too advanced. The difference in size between the holotype of *T. peyeri* (PIMUZ T 3925) and PIMUZ A/I 2985, however, is the only observable character that allows one to distinguish between both forms. In the absence of qualitative diagnostic character, we prefer for the moment to refer both new specimens PIMUZ A/I 2985 and PIMUZ A/I 1959 to *Ticinepomis* cf. *T. peyeri*.

5.2 Phylogenetic analysis

The phylogenetic relationships of *Ticinepomis* have been much debated. Rieppel (1980) first compared this taxon with *U. picena*, a species from the Upper Triassic of Italy described by Costa (1862) and Bassani (1896). Cloutier (1991) included for the first time *Ticinepomis* in a computerized phylogenetic analysis. *Ticinepomis* was resolved as the sister-taxon to ((*Axelia* + *Wimania*) *Coelacanthus*). Forey (1998) observed that *Ticinepomis* brought instability in his analysis of coelacanth relationships, and consequently excluded it. Similarly, Wen et al. (2013) did not include it in their analysis, which comprises two new Chinese taxa, *Luopingcoelacanthus* and *Yunnancoelacanthus*. Dutel et al. (2012) re-included *Ticinepomis* in their analysis, and resolved it as basalmost latimeriids. According to these authors, the latimeriids relationships are as follow: ((((((*Swenzia* + *Latimeria*) *Macropoma*) *Undina*) *Holophagus*) (*Libys* + *Megalocoelacanthus*)) *Ticinepomis*). We performed a new phylogenetic analysis on the basis of the character matrix of Dutel et al. (2012), which is based on Forey's (1998) matrix with additional data from Friedman and Coates (2006) and the addition of *Megalocoelacanthus* to the matrix. Also included are both Middle Triassic Chinese taxa, *Luopingcoelacanthus* and *Yunnancoelacanthus* (Wen et al. 2013), and furthermore, we added some character's states for *T. peyeri* based on the redescription of the holotype and on the material described here because is referred to *Ticinepomis* cf. *T. peyeri*. Definitions of characters and the data matrix are available in Electronic Supplementary Material 1.

The parsimony analysis produced 1,288 equally most parsimonious trees (length = 306; consistency index = 0.3922; retention index = 0.6737), with a large polytomy for most of the Early Triassic terminal taxa (Fig. 9). *Ticinepomis* is resolved as the sister group of the pair *Garnbergia* + *Rebellatrix*, but this node is poorly supported by four homoplasies (36, 39, 55, 105), none of them being known in all three genera. Similarly, the node supporting the sister-pair *Garnbergia* + *Rebellatrix* is supported by a single homoplasy (98). In our analysis, *Latimeria* is the sister genus of the clade *Ticinepomis* (*Garnbergia* + *Rebellatrix*) but the node is weakly supported by five homplasies (2, 27, 46, 50, 107), whose states are unknown in at least two of the terminal taxa for each of them. *Swenzia*, usually resolved as the sister-genus of *Latimeria* (Clément 2005; Geng et al. 2009; Dutel et al. 2012; Wen et al. 2013), is here located as the sister genus of the clade *Latimeria* (*Ticinepomis* (*Garnbergia* + *Rebellatrix*)) based on three homoplasies

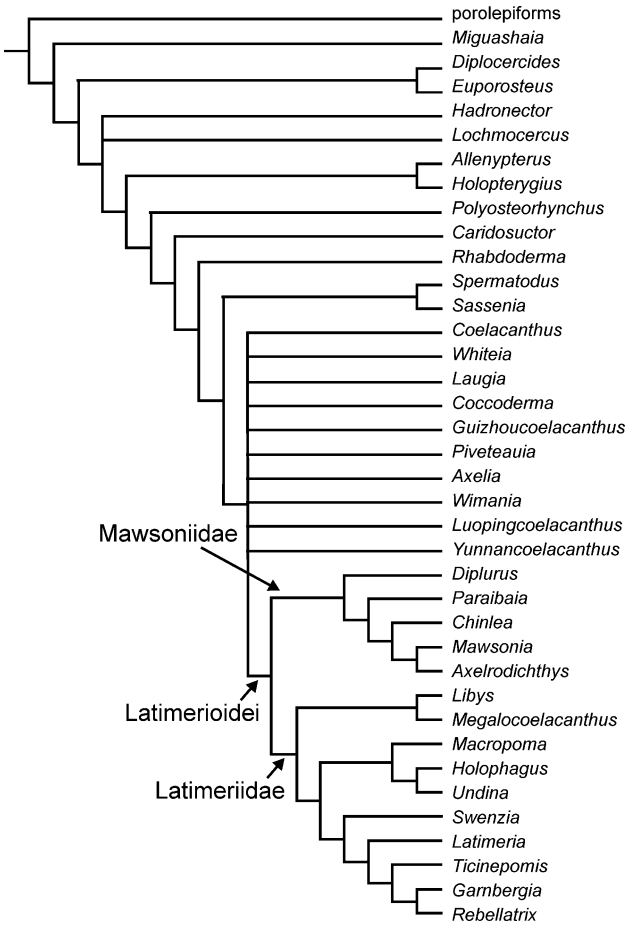

Fig. 9 Actinistian phylogeny based on the strict consensus tree of 1,288 equally most parsimonious trees (length = 306; consistency index = 0.3922; retention index = 6,737)

(26, 28, 30). This clade and a clade gathering *Macropoma* (*Holophagus* + *Undina*) are united by a node supported by four homoplasies (9, 59, 67, 74). Noteworthy, this clade and its sister clade *Libys* + *Megalocoelacanthus* are grouped on the basis of seven characters (2, 3, 22, 30, 39, 60, 110), three of them being uniquely derived characters: presence of an anterior branch of supratemporal commissure (22), presence of a subopercular branch of the mandibular sensory canal (60) and presence of a ventral swelling of the palatoquadrate (110). This node corresponds to the Latimeriidae as defined by Dutel et al. (2012), and our new observations allow to confirm that two of the above mentioned synapomorphies, presence of a subopercular branch of the mandibular sensory canal (60) and presence of a ventral swelling of the palatoquadrate (110), are actually present in *Ticinepomis*. Latimeriidae form the sister group of Mawsoniidae, whose content and definition are similar to those of Dutel et al. (2012). The main differences of our analysis with those of Dutel et al. (2012) are: (1) the position of *Ticinepomis*, which is no more the sister group of all other latimeriids, but nested within the family; (2) the inclusion of *Garnbergia* and *Rebellatrix* within the latimeriids; and (3) the intrarelationships of terminal taxa within the latimeriids, in particular the relationships between *Latimeria*, *Swenzia* and *Macropoma*. However, as mentioned above, most of the intra-nodes of latimeriids are weakly supported. Consequently, we regard the pattern proposed here as tentative.

We also calculated the 50 % majority-rule tree, which displays a better resolution for the Triassic genera than the strict consensus tree (Fig. 10). The phylogenetic relationships of non-latimerioid genera is similar to the pattern obtained by Dutel et al. (2012), except for the position of *Coelacanthus*, located in a more basal position in our analysis, and for the position of *Whiteia*, *Guizhoucoelacanthus* and *Piveteauia*, which form a clade with *Wimania* and *Axelia* in the analysis of Dutel et al. (2012), while they are located in pectinated positions, basal to the pair of genera *Wimania* + *Axelia*, in our analysis. Although the set of

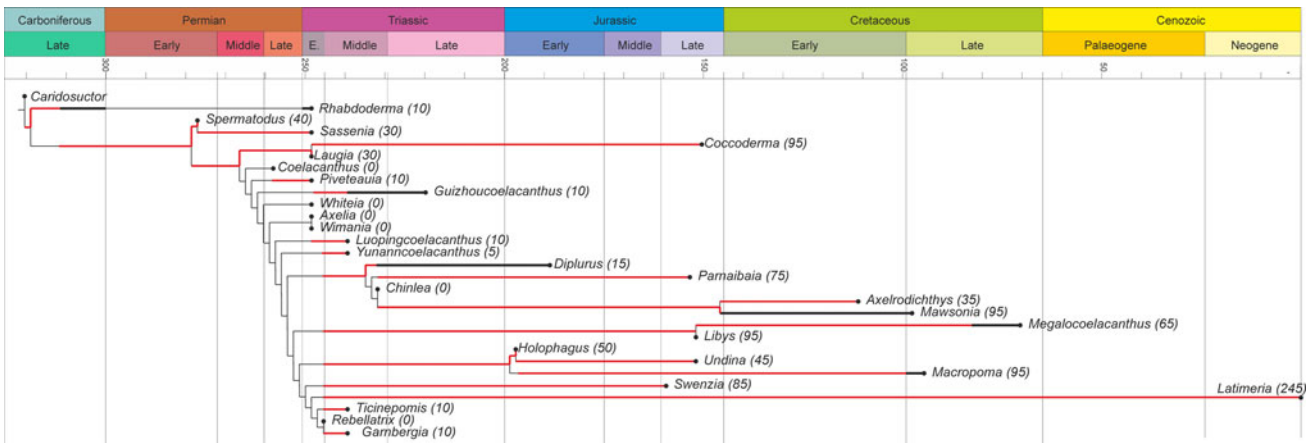

Fig. 10 50 % majority-rule calibrated tree of Mesozoic coelacanth genera (plus a few Palaeozoic taxa to compute Fig. 11). The phylogenetic pattern is in *black* and ghost lineages are in *red*. *Number in brackets* represents the ghost duration for each taxon, in millions years (approximation at 5 millions years)

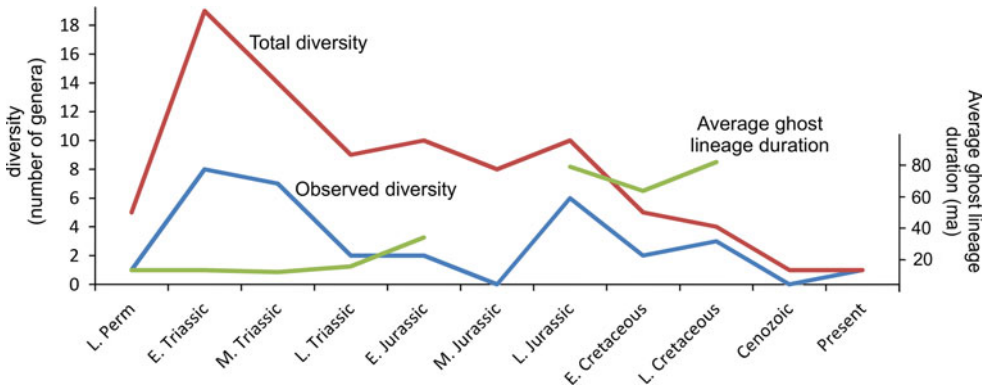

Fig. 11 "Observed diversity" (*blue*) in number of genera, "total diversity" (*red*) including "observed diversity" plus Lazarus taxa and ghost lineages, and average ghost lineage duration (*green*) for the coelacanths from the Late Permian to the present (in millions years). The value of the average ghost lineage duration for Present, not shown on the graph, equals 245 ma. See text for further explanation. *E* Early, *M* Middle, *L* Late

terminal taxa is not exactly the same in the analysis of Geng et al. (2009), their 50 % majority-rule tree is in accordance with the analysis of Dutel et al. (2012). Eventually, as in the 50 % majority-rule tree calculated by Wen et al. (2013), *Yunnancoelacanthus* and *Luopingcoelacanthus* in our analysis are located in pectinated basal position relatively to the latimerioids.

5.3 Diversity of post-Palaeozoic coelacanths

All previous studies that analysed coelacanth diversity through time (Cloutier 1991; Forey 1998; Schultze 2004; Wen et al. 2013) detected the highest peak of taxic diversity in the Early Triassic, and the second highest peak in the Late Jurassic. This pattern is also observed in the present study with high peaks of observed diversity in the Early Triassic and in the Late Jurassic (Fig. 11). The inclusion of ghost lineages in the calculation of the diversity curved, inferred from the 50 % majority-rule tree (Fig. 10), and called here the 'total diversity', slightly alters the initial pattern by smoothing the curve. The Early Triassic peak is still observed but the Late Jurassic peak is almost erased. Then, the total diversity curve regularly drops down to the present. More interesting is to compare this diversity curve with the curve of average ghost lineage duration. The Early Triassic peak of diversity is associated with very low average ghost lineage duration, suggesting that a biological radiation occurred at that time or slightly before, i.e. that most of the Early Triassic taxa are located at the extremity of stratigraphically short branches (10 ma in average). Wen et al. (2013) have recently suggested that coelacanths were disaster taxa and, thanks to their ability to dwell in dysoxic and anoxic environments, they were able to radiate in the aftermath of the end-Permian mass extinction. To the contrary of the Early Triassic peak, the Late Jurassic peak of diversity is associated with a high average, ghost lineage duration (82 ma in average). Consequently, we regard the Late Jurassic peak of observed diversity as caused by a Lagerstätten effect, in particular due to the very rich, classical Plattenkalk localities from Bavaria, Germany. A similar pattern, i.e., observed high diversity and high average ghost lineage duration, was observed for the Late Jurassic ray-finned fish, indicating that this peak of diversity is also an artefact of preservation (Cavin 2010). The average ghost lineage duration of coelacanths shows a constant increase since the Late Triassic (with a gap in the Middle Jurassic caused by the absence of considered coelacanth material in this time interval), which reaches its maximum in the fossil record in the Late Cretaceous. This pattern indicates that Cretaceous genera are representative of old lineages, with few diversification events. Today, the single coelacanth genus *Latimeria* has a ghost lineage of circa 245 ma according to the present phylogeny, making it one of the vertebrate genera located on the longest isolated branch of the tree of life together with the Australian lungfish *Neoceratodus* (Cavin and Kemp 2011).

6 Conclusions

The two specimens described in this paper are the first coelacanths to be recorded from the Prosanto Formation and the Middle Triassic of the Austroalpine realm. The vertebrate assemblage from the Prosanto Formation is dominated by ray-finned fishes, as is the assemblage of the Besano Formation in Monte San Giorgio. Both specimens from the Prosanto Formation show close affinities with the holotype specimen of *T. peyeri* from the Besano Formation, and we refer the material from Graubünden to *Ticinepomis* cf. *T. peyeri*. However, because the new specimen only shows the ventral part of the head, it is

possible that further discoveries will question this assignment. The new material of *Ticinepomis* allowed us to add new morphological characters to the available data matrix of coelacanths, and the parsimony analysis of this matrix supports the resolution of this genus as nested within the Latimeriidae. A global analysis shows that the generic diversity of coelacanths exploded in the Early Triassic. In the Middle Triassic, their generic diversity decreased, although the inclusion of ghost lineages in the analysis shows that the drop is not as sharp as previously supposed.

Acknowledgments This article is dedicated to our friend and colleague, the late Prof. Jean-Pierre Berger, for his important research in the field of palaeontology, and for spreading the palaeontological science to a broad audience. The Palaeontological Institute and Museum, University of Zürich (PIMUZ) enabled H.F. the systematic prospection and numerous excavations near Davos. The government of Canton Graubünden, and the Bündner Naturmuseum in Chur gave the permission for the excavations and financial support. Markus Hebeisen (PIMUZ) carefully prepared the first specimen (caudal fin). Max Kuhn (Uster) provided generous financial support for the preparation of the second, sub-complete specimen by C.O. This study was partly funded by the Swiss National Science Foundation for LC (200021-140827). We thank Isabelle Santoro and Colette Hamard, from the Musée d'Art et d'Histoire de la Ville de Genève, for the X-rays photographs of a specimen. We also thank Marius Hublard (Ilanz) and Benjamin Jost (Zürich), who drawed the geological figures, as well as Laura Wilson (University of New South Wales, Kensington NSW 2052, Australia) who improved the English, Hugo Dutel (Paris) and an anonymous reviewer, who provided valuable comments and critics, as well as Daniel Marty for his editorial work.

References

Anthony, J., & Robineau, D. (1976). Sur quelques caractères juvéniles de *Latimeria chalumnae* Smith (Pisces, Crossopterygii, Coelacanthidae). *Comptes Rendus de l'Académie des Sciences, Paris Série D, 283*, 1739–1742.

Arratia, G., & Herzog, A. (2007). A new halecomorph fish from the Middle Triassic of Switzerland and its systematic implications. *Journal of Vertebrate Paleontology, 27*, 838–849.

Arratia, G., Schultze, H.-P., & Casciotta, J. (2001). Vertebral column and associated elements in Dipnoans and comparison with other fishes: development and homology. *Journal of Morphology, 250*, 101–172.

Bassani, F. (1896). L'ittiofana della Dolomia Principale di Giffoni. *Palaeontographia italica, 1*, 169–210.

Bellotti, C. (1857). Descrizione di alcune nuove specie di pesci fossili di Perledo e d'altre località lombarde. In A. Stoppani (Ed.), *Studi geologici e paleontologici sulla Lombardia* (pp. 419–438). Milano.

Beltan, L. (1972). La faune ichthyologique du Muschelkalk de la Catalogne. *Memorias de la Real Academia de Ciencias y Artes de Barcelona, Tercera Epoca, 41*, 280–325.

Brito, P. M., & Martill, D. M. (1999). Discovery of a juvenile coelacanth in the lower Cretaceous, Crato formation, Northeastern Brazil. *Cybium, 23*, 311–314.

Bürgin, T. (1999). Middle Triassic marine fish faunas from Switzerland. In G. Arratia & H.-P. Schultze (Eds.), *Mesozoic Fishes 2: Systematics and the Fossil Record* (pp. 481–494). München: Verlag Dr. Friedrich Pfeil.

Bürgin, T., Eichenberger, U., Furrer, H., & Tschanz, K. (1991). Die Prosanto-Formation—eine fischreiche Fossil-Lagerstätte in der Mitteltrias der Silvretta-Decke (Kanton Graubünden, Schweiz). *Eclogae Geologicae Helvetiae, 84*, 921–990.

Bürgin, T., & Herzog, A. (2002). Die Gattung *Ctenognathichthys* (Actinopterygii; Perleidiformes) aus der Prosanto-Formation (Ladin, Mitteltrias) Graubündens (Schweiz), mit der Beschreibung einer neuen Art, *C. hattichi* sp. nov. *Eclogae Geologicae Helvetiae, 95*, 461–469.

Cavin, L. (2010). The Late Jurassic ray-finned fish peak of diversity: biological radiation or preservational bias? In J. S. Nelson, H.-P. Schultze, & M. V. H. Wilson (Eds.), *Origin and phylogenetic interrelationships of teleosts honoring Gloria Arratia* (pp. 111–121). München: Verlag Dr. Friedrich Pfeil.

Cavin, L., & Forey, P. L. (2007). Using ghost lineages to identify diversification events in the fossil record. *Biology Letters, 3*, 201–204.

Cavin, L., & Kemp, A. (2011). The impact of fossils on the evolutionary distinctiveness and conservation status of the Australian lungfish. *Biological Conservation, 144*, 3140–3142.

Clément, G. (2005). A new coelacanth (Actinistia, Sarcopterygii) from the Jurassic of France, and the question of the closest relative fossil to *Latimeria*. *Journal of Vertebrate Paleontology, 25*, 281–291.

Cloutier, R. (1991). Patterns, trends, and rates of evolution within the Actinistia. *Environmental Biology of Fishes, 32*, 23–58.

Cloutier, R. (2010). The fossil record of fish ontogenies: insights to developmental patterns and processes. *Seminars in Cell and Developmental Biology, 21*, 400–413.

Costa, O. G. (1862). Studii sopra i terreni ad ittioliti del Regno di Napoli. *Estratti dall'appendice agli atti della R. Accademia delle Scienze di Napoli, 12*, 1–44.

Dutel, H., Maisey, J. G., Schwimmer, D. R., Janvier, P., Herbin, M., & Clément, G. (2012). The giant Cretaceous Coelacanth (Actinistia, Sarcopterygii) *Megalocoelacanthus dobiei* Schwimmer, Stewart and Williams, 1994, and its bearing on Latimerioidei interrelationships. *PLoS ONE, 7*, e49911. doi:10.1371/journal.pone.0049911.

Forey, P. L. (1981). The coelacanth *Rhabdoderma* in the Carboniferous of the British Isles. *Palaeontology, 24*, 203–229.

Forey, P. L. (1998). *History of the coelacanth fishes* (p. 419). London: Chapman and Hall.

Fraser, N.C., Furrer, H.A. (2013). New species of *Macrocnemus* from the Middle Triassic of the Eastern Swiss Alps. *Swiss Journal of Geosciences*. doi:10.1007/s00015-013-0137-5.

Friedman, M., & Coates, M. I. (2006). A new recognized fossil coelacanth highlights the early morphological diversification of the clade. *Proceedings of the Royal Society, Series B, 273*, 245–250.

Furrer, H. (1995). The Prosanto Formation, a marine Middle Triassic Fossil-Lagerstätte near Davos (Canton Graubünden, Eastern Swiss Alps). *Eclogae Geologicae Helvetiae, 88*, 681–683.

Furrer, H. (2009). So kam der Fisch auf den Berg—Eine Broschüre über die Fossilfunde am Ducan. *Bündner Naturmuseum Chur und Paläontologisches Institut und Museum Universität Zürich, 2*. aktualisierte Auflage (pp. 32).

Furrer, H., Eichenberger, U., Froitzheim, U., & Wurster, D. (1992). Geologie, Stratigraphie und Fossilien der Ducankette und des Landwassergebiets (Silvretta-Decke, Ostalpin). *Eclogae Geologicae Helvetiae, 85*, 245–256.

Furrer, H., Schaltegger, U., Ovtcharova, M., & Meister, P. (2008). U-Pb zircon age of volcanic layers in Middle Triassic platform carbonates of the Austroalpine Silvretta nappe (Switzerland). *Swiss Journal of Geosciences, 101*, 595–603.

Geng, B.-H., Zhu, M., & Jin, F. (2009). A revision and phylogenetic analysis of *Guizhoucoelacanthus* (Sarcopterygii, Actinistia) from the Triassic of China. *Vertebrata PalAsiatica, 47*, 311–329.

Grauvogel-Stamm, L., Meyer-Berthaud, B., & Vozenin-Serra, C. (2003). Conifer axes from the Middle Triassic of Switzerland: structure and affinities. *Courier Forschungsinstitut Senckenberg, 241*, 51–67.

Herzog, A. (2001). *Peltoperleidus obristi* sp. nov., ein neuer, kleiner Strahlenflosser (Actinopterygii, Perleidiformes) aus der Prosanto-Formation (Mitteltrias) von Graubünden (Schweiz). *Eclogae Geologicae Helvetiae, 94*, 495–507.

Herzog, A. (2003a). Eine Neubeschreibung der Gattung *Eoeugnathus* Brough, 1939 (Actinopterygii; Halecomorphi) aus der alpinen Mitteltrias Graubündens (Schweiz). *Paläontologische Zeitschrift, 77*, 201–218.

Herzog, A. (2003). Die Knochenfische der Prosanto-Formation (Mitteltrias, GR)—Systematik, Funktionsmorphologie und Paläökologie. *PhD Dissertation* (pp. 330). Zürich: Universität Zürich.

Johanson, Z., Long, J., Talent, J., Janvier, P., & Warren, J. (2006). Oldest coelacanth, from the Early Devonian of Australia. *Biology Letters, 2*, 443–446.

Maddison, D. R. (1991). The discovery and importance of multiple islands of most-Parsimonious trees. *Systematic Zoology, 40*, 315–328.

Martin, M., & Wenz, S. (1984). Découverte d'un nouveau Coelacanthidé, *Garnbergia ommata* n.g., n.sp., dans le Muschelkalk supérieur du Baden-Württemberg. *Stuttgarter Beiträge zur Naturkunde. Serie B (Geologie und Paläontologie), 105*, 1–17.

Reis, O. M. (1888). Die Coelacanthinen, mit besonderer Berücksichtigung der im Weissen Jura Bayerns vorkommenden Gattungen. *Palaeontographica, Stuttgart, 35*, 1–96.

Rieppel, O. (1980). A new coelacanth from the Middle Triassic of Monte San Giorgio, Switzerland. *Eclogae Geologicae Helvetiae, 73*, 921–939.

Rieppel, O. (1985). A second actinistian from the Middle Triassic of Monte San Giorgio, Kt. Tessin, Switzerland. *Eclogae Geologicae Helvetiae, 78*, 707–713.

Schaeffer, B., & Gregory, J. T. (1961). Coelacanth fishes from the continental Triassic of the western United States. *American Museum Novitates, 2036*, 1–18.

Scheyer, T. M., & Desojo, J. B. (2011). Palaeohistology and external microanatomy of rauisuchian osteoderms (Archosauria: Pseudosuchia). *Palaeontology, 54*, 1–14.

Schultze, H.-P. (1972). Early growth stages in coelacanth fishes. *Nature, 23*, 90–91.

Schultze, H.-P. (1980). Eier legende und lebend gebärende Quastenflosser. *Natur und Museum, 110*, 101–108.

Schultze, H.-P. (2004). Mesozoic sarcopterygians. In G. Arratia & A. Tintori (Eds.), *Mesozoic fishes 3—systematics, paleoenvironments and biodiversity* (pp. 463–492). München: Verlag Dr. Friedrich Pfeil.

Schweizer, R. (1966). Ein Coelacanthide aus dem Oberen Muschelkalk Göttingens. *Neues Jahrbuch für Geologie und Paläontologie, Abhandlungen, 125*, 216–226.

Smith, J. L. B. (1939). A living fish of Mesozoic type. *Nature, 143*, 455–456.

Stockar, R., Baumgartner, P., & Condon, D. (2012). Integrated Ladinian biochronostratigraphy and geochrononology of Monte San Giorgio (Southern Alps, Switzerland). *Swiss Journal of Geosciences, 105*, 85–108.

Swofford, D. L. (2001). *PAUP*: phylogenetic analysis using parsimony and other methods (software).* Sunderland: Sinauer Associates.

Watson, D. M. S. (1927). The reproduction of the coelacanth fish, Undina. *Proceedings of the Zoological Society of London, 1927*, 453–457.

Wen, W., Zhang, Q.-Y., Hu, S.-X., Benton, M. J., Zhou, C.-Y., Tao, X., et al. (2013). Coelacanths from the Middle Triassic Luoping Biota, Yunnan, South China, with the earliest evidence of ovoviviparity. *Acta Palaeontologica Polonica, 58*, 175–193. doi:10.4202/app.2011.0066.

Wendruff, A. J., & Wilson, M. V. H. (2012). A fork-tailed coelacanth, *Rebellatrix divaricerca*, gen. et sp. nov. (Actinistia, Rebellatricidae, fam. nov.), from the lower Triassic of Western Gondwana. *Journal of Vertebrate Paleontology, 32*, 499–511.

Witzmann, F., Dorka, M., & Korn, D. (2010). A juvenile Early Carboniferous (Viséan) coelacanth from Rösenbeck (Rhenish Mountains, Germany) with derived postcranial characters. *Fossil Record, 13*, 309–316.